9.3 RADIATIVE COOLING OF STRATOCUMULUS

Hermann Gerber*
Gerber Scientific, Inc., Reston, VA

Szymon Malinowski
University of Warsaw, Warsaw, Poland

Anthony Bucholtz
Naval Research Laboratory, Monterey, CA

Tyler Thorsen
University of Washington, Seattle, WA

1. INTRODUCTION

The importance of the large fields of stratocumulus clouds (Sc) along the western margins of continents to the radiation budget of our planet is well established. Thus it is essential to predict accurately the behavior of Sc in order to contribute properly to models dealing with climate change. Understanding physical processes associated with Sc is a necessary first step needed for accurate predictions. Although a large amount of literature exists describing many field campaigns and modeling efforts dealing with Sc, there are still existing uncertainties about Sc processes that have strong bearing on their behavior.

An aircraft field campaign of six years ago termed POST (Physics of Stratocumulus Top; Gerber, 2010) consisted of 17 flights in unbroken Sc off the California Coast. The main emphasis of POST was on understanding better the entrainment process (Malinowski et al., 2011, 2013; Chuang et al., 2012; Gerber et al., 2013). The POST aircraft, a Twin Otter from CIRPAS (Naval Postgraduate School for Interdisciplinary Remotely Piloted Aircraft Studies), also included pyrgeometers and pyranometers mounted on top and bottom of the aircraft fuselage making it possible to calculate radiative flux divergence and cooling rate due to LW (infrared) radiation. Measurements with other sensors on the aircraft also produced direct values of the cooling rate. This paper takes an initial look at these cooling rates for two POST flights, compares them to a current radiation transfer model, and comments on the status of such measurements.

It is well accepted that warm Sc behave essentially as radiative black bodies in the infrared, and that strong radiative cooling occurs near cloud top causes negative buoyancy that drives the larger-scale circulation in the Sc. Much has been written about the LW interaction with warm Sc. The pioneering papers in the late 1970s and in the 1980s on LW cooling-rate measurements by colleagues in the British Met Office are especially noteworthy in describing radiation-Sc interactions. (Pollard, 1978, Slingo et al., 1982a, 1982b; Nicholls, 1984). Later field Sc campaigns with LWC cooling rate estimates include those by Curry and Herman (1985) and by Kawa and Pearson (1989). In addition modeling studies of Sc cooling rates include Roach and Slingo (1979), Curry and Herman (1985), Davies and Alves (1989), Fu and Liou (1992), Kruerger et al. (1995), and Stevens et al. (2005). All these studies show the expected strong cooling rate near Sc cloud top. However, the rates differ substantially in magnitude near cloud top and in their distribution within the Sc. It is not clear if these differences are only a result of using different atmospheric parameters that affect the cooling measurements and modeling, or if systematic errors also play a role. A current radiation transfer code (Fu and Liou, 1992; Rose and Charlock, 2002) permits a full range of relevant inputs as described in http://snowdog.larc.nasa.gov/cgibin/rose/-flp200503/flp200503.cgi.

The present analysis of pyrgeometer data from the POST campaign differs from those made previously in that LW cooling rates are estimated near Sc top for periods on the order of hours as the aircraft flew a quasi-Lagrangian pattern following the advection of the Sc, and in that improved sensors were used. The following describes relevant instruments used on the aircraft, measurements, cooling rates from the two POST flights, comparison with the Fu-Liou radiation transfer code, and conclusions and suggestions.

* *Corresponding author address*: H. Gerber, Gerber Scientific, Inc., Reston, VA 20190; email: hgerber6@comcast.net

2. EXPERIMENTAL

2.1 *Instrumentation*

Three different instruments produced data used in this study. The first are Kipp & Zonen aircraft-modified CG-4 pyrgeometers with a wavelength sensitivity range from 4.5 m to 42 m (Bucholtz et al., 2010). The response time of these pyrgeometers published by the manufacturer is 8 s. The pyrgeometers were calibrated at the NRL facility located at CIRPAS; and their accuracy is estimated to be between 3% and 5%. The second instrument is the UFT-M (Ultra Fast Temperature probe, version M; Kumala et al., 2013) which is capable of high-resolution temperature measurements with a precision of a few tenths of one ^{0}C both incloud and out of cloud. The UFT-M is scaled using a dew-point hygrometer also located on the aircraft. The final instrument is the PVM-100A (Particulate Volume Monitor, aircraft version; Gerber et al.,1994) that produces LWC (liquid water content) high-rate measurements with an accuracy of 10% for droplet diameter up to ~35 m; the PVM also measures Re (droplet effective radius) over a range from ~ 3 m to ~12.5 m. The UFT-M and PVM were mounted within 0.5 m near the nose of the Twin Otter aircraft. Given the relatively slow response time of the pyrgeometers, 1-hz UFT-M and PVM-100 data are used in the following.

2.2 *Aircraft Deployment*

Figure 1 shows a satellite image of Sc over the Pacific Ocean near the coast of California during POST flight TO3 (7/19/2008, UTC). The sketched lines show the typical flight path of the Twin Otter used during POST, with the solid line showing a horizontal zig-zag pattern during which data were collected. This pattern can be called quasi-Lagrangian in that it progresses at a rate that matches the mean speed and direction in the Sc as given by the white arrow. The Sc were dissipating upwind of the TO3 flight path given dry air blowing from the NNE off the continent.

Figure 2 shows a typical example of pyrgeometer and LWC measurements during vertical profiles made by the aircraft though Sc top over a period of 1000 s. These saw-tooth-like profiles ("porpoises") extended approximately 100-m above and below Sc top, and were conducted nearly all the time while the aircraft was making the horizontal zig zags. This resulted in a large number of profiles during each flight that lasted ~ 5 hrs. The profile ascend and descend rates were kept at ~1.5 m s^{-1}. Occasionally the aircraft would perform a deeper sounding both below and above cloud top. Here cloud top is defined as the height above which the LWC sensor on the aircraft first observes cloud free air on ascend, and first observes solid cloud on descend.

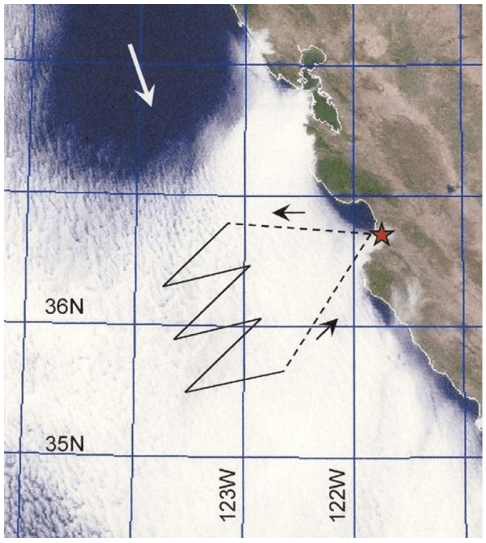

Fig. 1 - NexSat satellite image (courtesy Naval Research Laboratory, Monterey, CA) of the partially stratocumulus -covered Pacific Ocean near the California Coast during flight TO3 of the POST (Physics of Stratocumulus Top) aircraft field campaign. The CIRPAS Twin Otter aircraft flew from the airport in Marina, CA (red star) located next to Monterey Bay to an away point about 125 km from the coast. At that point it progressed in a zig-zag pattern matching the average velocity of the Sc field.

3. FLIGHT TO12

The LW cooling rate (^{0}C hr^{-1}) is usually calculated from pyrgeometer data using

$$\frac{\delta T}{\delta t} = \frac{1}{\rho c_p} \frac{\delta F_{net}}{\delta z}$$

where the vertical gradient of the net radiative flux F_{net} is given by the difference of the downward and upward fluxes (see Fig. 2) divided by the vertical increment z, is the atmospheric density, and c_p is the specific heat of air at constant pressure.

Figure 3 shows t for POST flight TO12 (8/8/2008, UTC) as a function of the vertical distance from cloud top. The upper plot represents data as the aircraft ascends, and the bottom plot shows data as the aircraft descends during the zig zag; a total of 52 penetrations of cloud top were made for flight TO12, with 26 represented in each plot in Fig. 3. Both plots show maximum t near cloud top as expected; however, significant

differences are seen. The portion above cloud top for the "porpoise up" data shows an approximate exponential decrease of t with height in contrast to that portion shown for the "porpoise down" data. The portions below cloud top also show differences with the "porpoise down" data showing a less rapid decrease of t. This behavior is interpreted as being due to the 8-s response time of the pyrgeometers which is illustrated in the upper plot where circles data representing an exponential decrease with a time constant of 1/e = 8s are shown. It appears that when the pyrgeometer on top of the aircraft fuselage leaves the cloud and first views the cold upper atmosphere the thermal time lag of the pyrgeometer is most evident. The same happens when this pyrgeometer enters the cloud where its exposure to the upper atmospheric radiation rapidly diminishes.

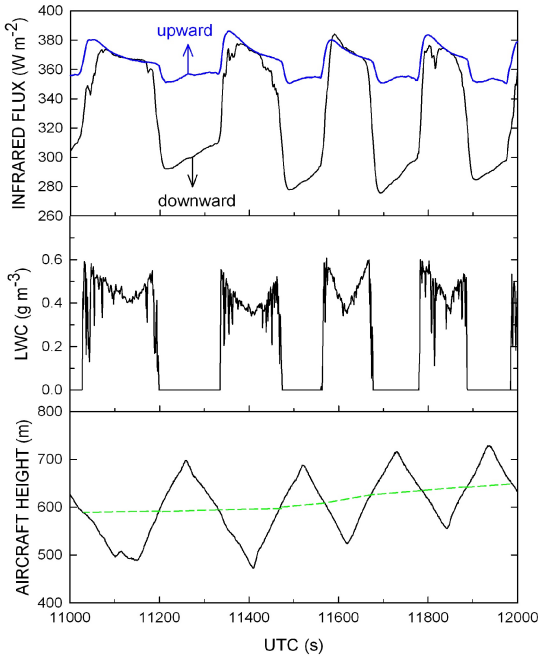

Fig. 2 - A 1000-s increment of flight TO12 showing flux outputs from the pyrgeometers located on the top (downward) and bottom (upward) of the aircraft fuselage. LWC was measured with the PVM probe. The aircraft flew multiple slant-path profiles ("porpoises") extending about 100-m above and below Sc top shown by the green dashed line.

In order to minimize the effect of the pyrgeometer thermal time lag we combine from Fig. 3 the t data from below cloud top from the "porpoise up" plot with the t data from above cloud top from the "porpoise down" plot to result in the final t plot for flight TO12 shown in Fig. 4. This procedure limits the exposure of the pyrgeometers to rapid changes of the LW radiation.

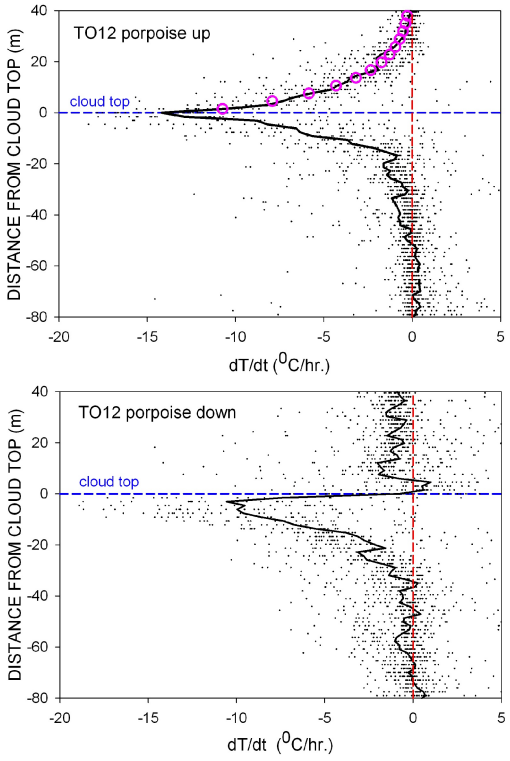

Fig. 3 - Cooling rates for flight TO12 as a function of height from cloud top derived from the pyrgeometer measurements for ascending (porpoise up) and descending (porpoise down) porpoises. All porpoises are referenced to cloud top defined as the upper limit of unbroken cloud. Each plot consists of 1-hz data (dots) for 26 ascends and descends; and the solid black line is the average of the 1-hz data. The pink circles show the 1/e response time of 8 s of the fuselage-top pyrgeometer during ascend. See the text for a discussion of the difference between the two plots.

Figure 4 shows 1-hz t pyrgeometer data (dots) as a function of vertical distance from cloud top (~1.5-m vertical resolution), and shows the average t for the whole flight (black curve). Also shown is the prediction from the Fu-Liou LW radiation code where the necessary input variables for the flight were obtained from other TO12 data up to a height of ~ 2 km; see Fig. 5. The inputs between ~2 km and 5 km came from a radiosonde profile launched from Oakland near the time of flight TO12, and the inputs above 15 km are for the midlatitude

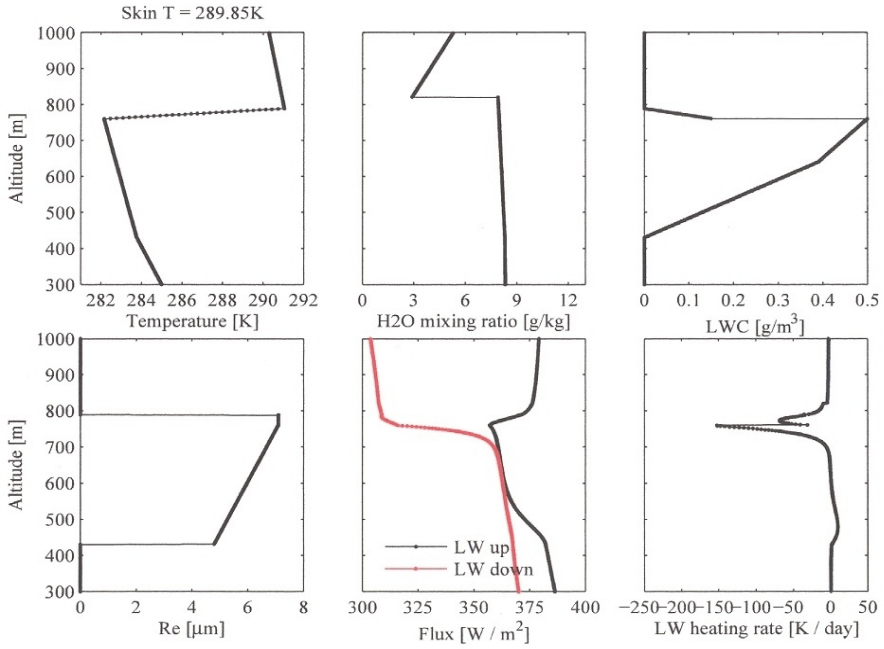

Fig. 5 - Temperature, water vapor, LWC, and effective radius (Re) curves based on fits to measured data on flight TO12 and used as inputs to the Fu-Lou radiation code. The bottom right two plots show code outputs.

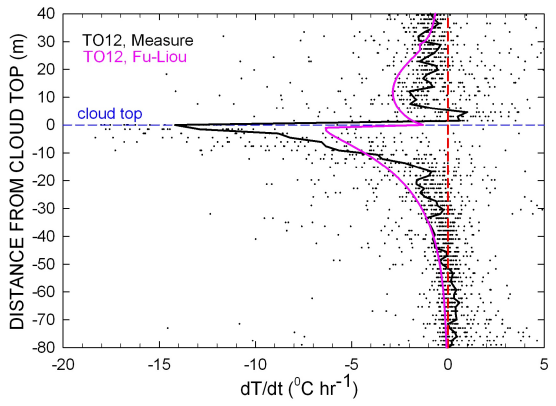

Fig. 4 - Cooling rates for flight TO12 combining the 26 "porpoise up" data from below cloud top with the 26 "porpoise down" data from above cloud top from Fig. 3 in order to reduce the thermal time lag of the pyrgeometers. The pink line is the prediction of the LWC cooling from the Fu-Liou radiation code (Fu and Liou, 1992.)

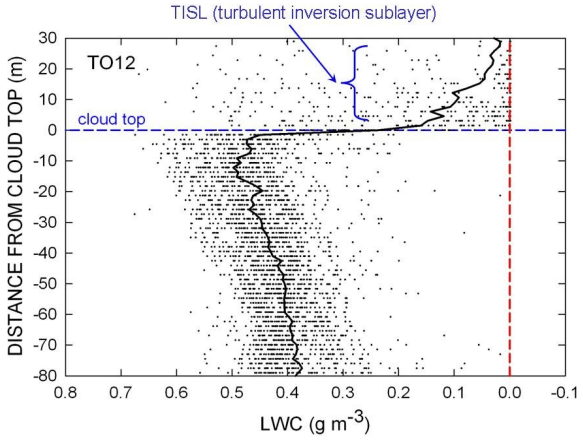

Fig. 6 - LWC measured during the 52 penetrations of Sc top during flight TO12 as a function of height near cloud top. The region above cloud top is a region of mixing and LWC evaporation termed TISL (Malinowski et al., 2013,)

summer profile. The average pyrgeometer prediction shows a larger cooling peak near cloud than the Fu-Liou calculated peak, with the latter also showing a more gradual decrease of *t* below cloud top; the former result was also found by Anthony Bucholtz (see Wang, et al., 2010). The vertical dependence of the measured *t* resembles more the vertical dependence of *t* shown by Davies and Alves (1989); and the dependence shows an approximate exponential decrease below cloud top. We also find that the peak 1-hz values of *t* near cloud top are approximately 2 times the average *t* value at cloud top. These peak values still may be an underestimate because of the slow response of the pyrgeometers.

Another feature of the pyrgeometer data is the presence of significant *t* cooling values (dots) below cloud top. An explanation for this feature is the presence of cloud parcels with reduced LWC. Slingo et al. (1982a) already showed such an effect where horizontal flight through their stratus encountered reduced LWC and enhanced radiative cooling. Further evidence of this effect is shown by Curry and Herman (1985). The Sc in flight TO12 were unbroken, and the reduced values of LWC were likely caused by entrainment of air from above cloud top. These cloud parcels with reduced LWC have been called “cloud holes” (Korolev and Mazin, 1993; also termed holes in the following) and have been characterized in detail (Gerber et al., 2005, 2013).

A final feature of the data in Fig. 4 is the presence of some radiative cooling above cloud top both in the measurements and in the Fu-Liou prediction. In the past, cause of such cooling has been attributed to the thermal response time of pyrgeometers. However, that does not appear to be the case here because the plot of LWC shown in Fig. 6 indicates the presence of a layer of rapidly decreasing values of LWC above cloud top. This layer has been described in detail by Malinowski et al. (2013), and is termed the TISL (turbulent inversion sub-layer). The many small measured values of LWC in this layer suggest that cloud water detrained from the Sc is in the process of evaporation. That amount of cloud water is apparently sufficient to cause the small amount of *t* cooling above cloud top as shown in Fig. 4.

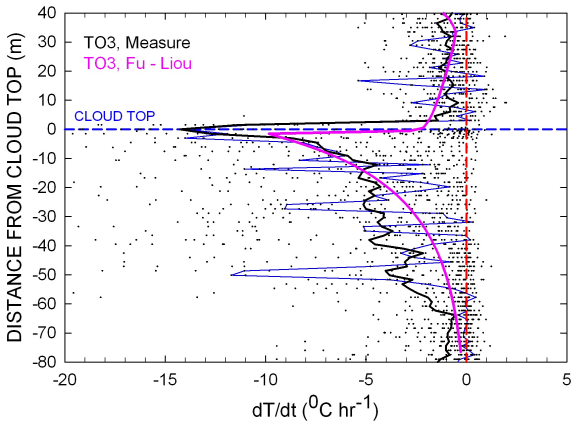

Fig. 7 - Cooling rates for flight TO3 as in Fig. 4. The blue solid lines are the cooling rates for one slant ascend/descend of the aircraft. See text for a discussion of the differences between Figs. 4 and 7.

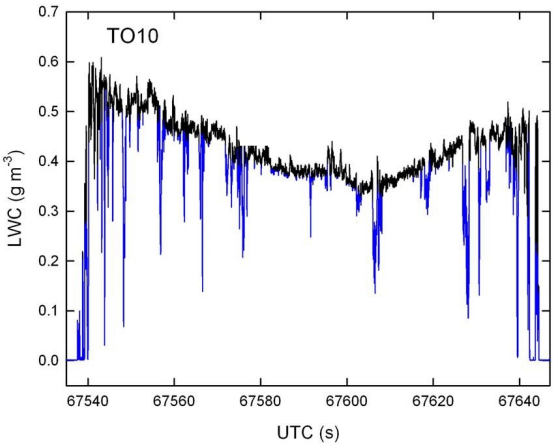

Fig. 8 - One porpoise down and up through an unbroken Sc showing LWC measurements as a function of time. Blue lines superimposed on the black lines are assumed to be cloud portions with reduced LWC (“cloud holes”) caused by the entrainment process (from Gerber et al., 2013.)

4. FLIGHT TO3

The reduced *t* data for the second flight TO3 is shown in Fig. 7. Similar features as for flight TO12 are again seen: The 1-hz pyrgeometer data again exceeds the Fu-Liou prediction, some cooling is again found above cloud top, and a large number of 1-hz *t* data points with large cooling are again found below cloud top. A significant difference between the data for flights TO12 and TO3 is the shape of the average data (solid black curves). This curve for TO3 no longer approximates exponential decrease below cloud top, but now shows significantly larger contributions to cooling below cloud top. The measured cooling is about twice the Fu-Liou predicted cooling rate over a relatively deep layer below cloud top. The difference in the vertical distribution of cooling between the two flights is likely related to the difference in the entrainment process for the two flights. TO12 has a modest entrainment rate and a moist layer above cloud top, while TO3 has a large value of

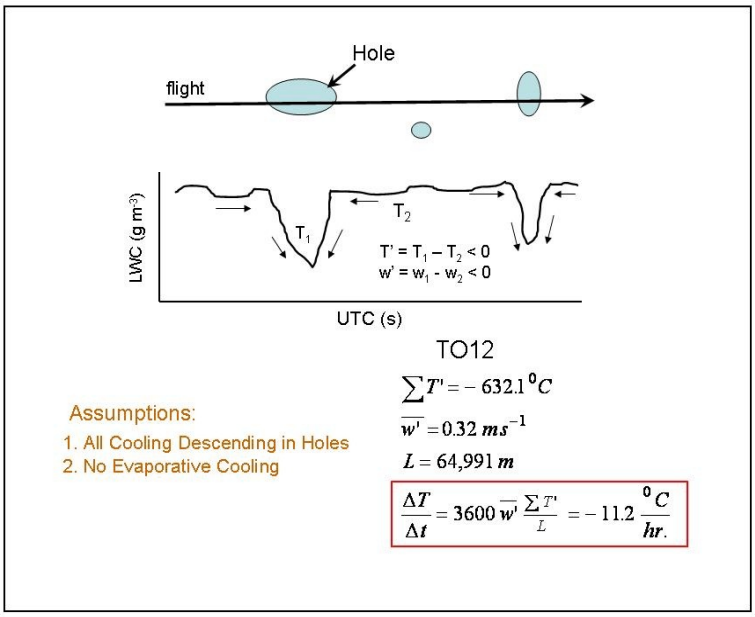

Fig. 9 - Schematic of aircraft flight through "cloud holes" and the corresponding LWC vs time (upper part of fig.) showing entrained air converging in the holes, and showing the definitions of temperature *T'* and vertical velocity *w'* in the holes. The bottom part gives assumptions needed to make the direct estimate of the cooling rate for flight TO12, and shows the observed numerical values needed to calculate *T/Dt* with the given equation.

entrainment due to strong cloud-top mixing caused by large directional wind shear and a dry layer located above cloud top. These differences between the two flights illustrate that omitting other physical processes near cloud top such as, for example, entrainment and wind shear leads to differences with the predicted LW cooling rates.

A blue curve added to Fig. 7 represents the *dT/dt* 1-hz data for one TO3 slant profile. The strong variation in the data represents the highly varying LWC values in this strongly entraining Sc. The peak cooling values of the blue data as well as of the other 1-hz data (dots) are highly correlated to reduced LWC values (not shown) in the holes.

5. DIRECT MEASURE OF *dT/dt*

A means exists to directly estimate the LW cooling rate from properties measured in the holes. Figure 8 illustrates such holes in one porpoise down and up through a Sc. The black curve shows measured background LWC values, while the blue curves that overlay the black curve show the presence of reduced LWC assumed to be caused by entrainment. The holes are readily identifiable and appear in all POST Sc. The cooling in the holes is given by

$$\frac{\delta T}{\delta t} = 3600\,\overline{w'}\,\frac{\sum T'}{L}$$

where the RHS of the equation represents the average flux of sensible heat removed from cloud top by the holes. The primed values are the mean differences in vertical velocity *w* and temperature *T* measured by the UFT-M between the holes and the cloud not affected by entrainment, and *L* is the horizontal aircraft distance over which the measurements are made.

Fig. 9 show a schematic for the use of the holes to directly calculate *dT/d t*, assumptions needed for this approach, numerical values for the measured parameters, and a resulting value of *dT/d t* for flight TO12. This direct value is reasonably close to the *dT/d t* value determined from the pyrgeometer flux-divergence approach for flight TO12 described in Section 3. The assumption that the

holes are not cooled by evaporative cooling of cloud water but rather result from radiative cooling is consistent with the conclusion of Nicholls (1989) who found evaporative cooling in Sc to be minimal, and is consistent with the recent UFT and LWC measurements in cloud holes described in Gerber et al (2013). Flight TO12 is suitable for such a direct estimate of *dT/d t*, because TO12 Sc show CTEI (buoyancy instability) near cloud top that causes the holes to descend.

6. CONCLUSIONS and SUGGESTIONS

This work describes estimates of the LW cooling rates derived from radiation data collected by pyrgeometers on the Twin Otter aircraft during the POST field campaign in unbroken Sc off the California Coast. A direct approach for estimating the rate is also described. This initial look at the POST data is for lengthy flights in two different Sc made in a quasi-Lagrangian manner so that average cooling rates for the cloud field are obtained. Also comparisons are made with cooling rates predicted by the Fu-Liou LW radiation code. This work resulted in the following major observations:

- Small LW cooling rates were found in a layer adjacent to cloud top. These rates appeared to be due to the "turbulent inversion sub-layer" where detrained cloud water was evaporating, rather than being due to the thermal time lag of pyrgeometers which has been an explanation in the past.

- There are two LW cooling rate regimes in the observed Sc. One produces an approximate exponential decrease of the cooling below Sc top, and the other is related to the presence of entrained parcels ("cloud holes") containing reduced LWC. The holes and their continued LW cooling can exist deep within the Sc. This must cause additional positive buoyancy generation that helps drive the larger Sc circulation, and which should be evaluated.

- The observed LWC cooling rates show a significantly larger cooling-rate peak near Sc top than does the prediction of the Fu-Liou radiation code. This result depends on the assumptions that the quoted accuracy of the pyrgeometers is correct, and that the procedure used here to combine portions of the measured LW fluxes is valid. Given that the observed rates depend on the relatively slow-response pyrgeometers used during the POST, the observed peak values are likely still underestimates of the true maximum values.

- Given the large differences in the vertical distribution of the cooling rates in the two Sc flights described here, suggests that physical processes near Sc top such as entrainment and wind shear should be represented in LW radiation transfer codes to produce more realistic cooling rates. Comparison of cooling rates for day and night Sc, where entrainment rates have large difference, is a simple thing to try for improving the codes. Other tries could include more complexities such as wind properties and TKE near cloud top. A more complete look than done here at the POST data base and existing POST publications can provide information for such tries.

- Up to this point all discussion has been about LW cooling rates. What is actually more desirable is to have cooling amounts that would be equivalent to time integrals of the cooling rates over time intervals when the cloud parcels are exposed to LW cooling. This applies especially to the observed cooling in the "cloud holes" which might have rather different time-dependent cooling rate histories. A LES study dealing with time-dependent LW cooling amounts would be desirable.

Acknowledgments

Appreciation is expressed to CIRPAS (Center for Interdisciplinary Remotely Piloted Aircraft Studies) for their excellent hosting of the POST field campaign, to Haflidi Jonsson the chief scientist of the Twin Otter aircraft for his many contributions to POST, and to Mike Hubbell the pilot who accurately flew the aircraft on all flight patterns desired by the POST P.I.'s. (POST was supported by the National Science Foundation and the Office of Naval Research.)

7. REFERENCES

Bucholtz, A., D.L. Hlavka, M.J., McGill, K.S. Schmidt, P. Pilewskie, S.M. Davis, E.A. Reid, and A.L. Walker, 2010: Directly measured heating rates of a tropical subvisible cirrus cloud. J. Geophys. Res., 115. D00Jo9, doi:10.1029/2009JD0113128.

Carman, J.K., D.L. Rossiter, D. Khelif, H.H. Jonsson, I.C. Faloona, and P.Y. Chuang, 2012: Observational constraints on entrainment and the entrainment interface layer in stratocumulus. *Atmos. Chem. Phys.*, 12, 11,135-11,152.

Curry, J.A., and G.F. Herman, 1985: Infrared radiative properties of summertime Arctic stratus clouds. *J. Climate Appl. Meteor.*, 24, 525-538.

Davies R., and A.R. Alves: Flux divergence of thermal radiation within stratiform clouds. *J. Geophys. Res.*, 94, 16,277-16,286.

Fu, Q., and K.N. Liou, 1992: On the correlated k-distribution method for radiative transfer in nonhomogenous atmospheres. *J. Atmos. Sci.*, 49, 2139-2156.

Gerber, H., B.G. Arends, and A.S. Ackerman, (1994): New microphysics sensor for aircraft use. *Atm. Res.*, 31, 235-252.

Gerber, H., S.P. Malinowski, J.-L. Brenguier, and F. Burnet, 2005: Holes and entrainment in stratocumulus. *J. Atmos. Sci.*, 62, 443-459.

Gerber, H., G. Frick, S.P. Malinowski, W. Kumala, and S. Krueger, 2010: POST - A new look at *stratocumulus.13th Conf. On Cloud Physics*,Portland, OR, 2010, Amer. Met. Soc., https://ams.confex.com/ams/13CldPhy13AtRad/webprogram/Paper170431.html

Gerber, H., G. Frick, S. P. Malinowski, H. Jonsson, D. Khelif, and S.K. Krueger, 2013: Entrainment rates and microphysics in POST stratocumulus. *J. Geophys. Res.*, 118, 1-16.

Kawa, S.R., and R. Pearson Jr., 1989: An observational study of stratocumulus entrainment and thermodynamics. *J. Atmos. Sci.*, 46, 2649-2661.

Korolev, A.V., and I.P. Mazin, 1993: Zones of increased and decreased droplet concentration in stratiform cloud. *J. Appl. Meteorol.*, 32, 760-773.

Krueger, S.K., G.T. McLean, and Q. Fu, 1995: Numerical simulation of the stratus - to cumulus transition in the subtropical marine boundary layer. Part I: Boundary-layer structure. *J. Atmos. Sci.*, 53, 2839-2850.

Kumala, W., K.E. Haman, M. Kopec, and S.P. Malinowski, 2013: Ultrafast thermometer UFT-M: High resolution temperature measurements during Physics of Stratocumulus Top [POST]. *Atmos. Meas. Tech.*, http://www.atmos-meas-tech.net/6/2043/amt-6-2043-2013.html

Malinowski, S.P., K.E. Haman, W. Kumala, and H. Gerber, 2011: Small-scale turbulent mixing at stratocumulus top observed by means of high-resolution airborne temperature and LWC measurements. *J. Phys. Conf. Ser.*, 318, doi:10.1088/1742-6596/318/7/072013

Malinowski, S.P., H. Gerber, I. Jen-LaPlante, M.K. Kopec, W. Kumala, K. Nurowska, and P.Y. Chuang, 2013: Physics of Stratocumulus Top (POST): turbulent mixing across capping inversion. *Atmos. Chem. Phys.*, 13, 15,233-15,269.

Nicholls, S., 1984: The dynamics of stratocumulus: aircraft observations and comparisons with a mixed layer model. *Quart. J. Roy. Meteor. Soc.*, 110, 783-820.

Nicholls, S., 1989: The structure of radiatively driven convection in stratocumulus. *Quart. J. Roy Meteor. Soc.*, 115, 487-511.

Pollard, R.T., 1978: The joint air-sea interaction experiment - JASIN 1978. *Bull. Amer. Meteor. Soc.*, 59, 1310-1318.

Roach, W.T., and A. Slingo, 1979: A high resolution infrared radiative transfer scheme to study the interaction of radiation with cloud. *Quart. J. Roy. Meteor. Soc.*, 105, 603-614.

Rose, F., and T. Charlock, 2002: New Fu-Liou code tested with ARM Raman lidar and CERES in pre-CALIPSO exercise. *Extended Abstracts*, 11th Conf. Atm. Rad., AMS, pp.3-7

Slingo, A., S. Nicholls, and J. Schmetz, 1982a: Aircraft observations of marine stratocumulus during JASIN. *Quart. J. Roy. Meteor. Soc.*, 108, 833-856.

Slingo, A., R. Brown, and C.L. Wrench, 1982b: A field study of nocturnal stratocumulus; III. High resolution radiative and microphysical observations. *Quart. J. Roy. Meteor. Soc.*, 108, 145-165.

Stevens, B., et al., 2005: Evaluation of large-eddy simulations via observations of nocturnal marine stratocumulus. *Month. Weather Rev.*, 133, 1443-1462.

Wang, S., Q. Wang, A. Bucholtz, and X. Zheng, 2010: Turbulence mixing in strongly sheared stratocumulus cloud topped marine boundary layer. Poster at *AGU Conf.*, San Francisco, CA.